

Modified aquila optimizer for forecasting oil production

Mohammed A. A. Al-qaness, Ahmed A. Ewees, Hong Fan, Ayman Mutahar AlRassas & Mohamed Abd Elaziz

To cite this article: Mohammed A. A. Al-qaness, Ahmed A. Ewees, Hong Fan, Ayman Mutahar AlRassas & Mohamed Abd Elaziz (2022) Modified aquila optimizer for forecasting oil production, Geo-spatial Information Science, 25:4, 519-535, DOI: [10.1080/10095020.2022.2068385](https://doi.org/10.1080/10095020.2022.2068385)

To link to this article: <https://doi.org/10.1080/10095020.2022.2068385>



© 2022 Wuhan University. Published by Informa UK Limited, trading as Taylor & Francis Group.



Published online: 10 May 2022.



Submit your article to this journal [↗](#)



Article views: 2462



View related articles [↗](#)



View Crossmark data [↗](#)



Citing articles: 25 View citing articles [↗](#)

Modified aquila optimizer for forecasting oil production

Mohammed A. A. Al-qaness ^a, Ahmed A. Ewees ^{b,c}, Hong Fan ^a, Ayman Mutahar AlRassas ^d
and Mohamed Abd Elaziz ^{e,f,g}

^aState Key Laboratory for Information Engineering in Surveying, Mapping and Remote Sensing, Wuhan University, Wuhan, China;

^bSystems, University of Bisha Department of e-, Bisha, Kingdom of Saudi Arabia; ^cDepartment of Computer, Damietta University, Damietta, Egypt; ^dSchool of Petroleum Engineering, China University of Petroleum (East China), Qingdao, China; ^eDepartment of Mathematics, Faculty of Science, Zagazig University, Zagazig, Egypt; ^fArtificial Intelligence Research Center (AIRC), Ajman University, Ajman 346, United Arab Emirates; ^gFaculty of Computer Science & Engineering, Galala University, Suze 435611, Egypt

ABSTRACT

Oil production estimation plays a critical role in economic plans for local governments and organizations. Therefore, many studies applied different Artificial Intelligence (AI) based methods to estimate oil production in different countries. The Adaptive Neuro-Fuzzy Inference System (ANFIS) is a well-known model that has been successfully employed in various applications, including time-series forecasting. However, the ANFIS model faces critical shortcomings in its parameters during the configuration process. From this point, this paper works to solve the drawbacks of the ANFIS by optimizing ANFIS parameters using a modified Aquila Optimizer (AO) with the Opposition-Based Learning (OBL) technique. The main idea of the developed model, AOOBL-ANFIS, is to enhance the search process of the AO and use the AOOBL to boost the performance of the ANFIS. The proposed model is evaluated using real-world oil production datasets collected from different oilfields using several performance metrics, including Root Mean Square Error (RMSE), Mean Absolute Error (MAE), coefficient of determination (R^2), Standard Deviation (Std), and computational time. Moreover, the AOOBL-ANFIS model is compared to several modified ANFIS models include Particle Swarm Optimization (PSO)-ANFIS, Grey Wolf Optimizer (GWO)-ANFIS, Sine Cosine Algorithm (SCA)-ANFIS, Slime Mold Algorithm (SMA)-ANFIS, and Genetic Algorithm (GA)-ANFIS, respectively. Additionally, it is compared to well-known time series forecasting methods, namely, Autoregressive Integrated Moving Average (ARIMA), Long Short-Term Memory (LSTM), Seasonal Autoregressive Integrated Moving Average (SARIMA), and Neural Network (NN). The outcomes verified the high performance of the AOOBL-ANFIS, which outperformed the classic ANFIS model and the compared models.

ARTICLE HISTORY

Received 4 August 2021
Accepted 3 March 2022

KEYWORDS

Oil production; ANFIS; opposition-based learning (OBL); Aquila Optimizer (AO); time series forecasting; Tahe oilfield; Sunah oilfield

1. Introduction

Forecasting oil production is crucial for petroleum engineers to alleviate the blind expenditure, ensure long-term development and maintain and monitor the life cycle of the oil reservoir. In addition, the reservoir parameters, including permeability, porosity, water saturation, type of crude oil, and reservoir heterogeneity, are considered the influence factors affecting the accuracy of forecasting oil production (Haider 2020). In the oil industry, various traditional approaches are employed to forecast oil production, including Numerical Reservoir Simulation (NRS) and Decline Curve Analysis (DCA) (Cumming 2013; Chong et al. 2017; Cancelliere, Verga, and Viberti 2011). NRS and DCA are the most common utilizing approaches to forecast oil production. However, these traditional approaches have limitations and obstacles to predict oil production accurately (Nwaobi and Anandarajah 2018). The application of NRS is presented as a reliable approach compared to the other conventional techniques. The NRS mainly depends on

the accuracy of the static geological model and the quality of history matching in the dynamic model (Hutahaeen, Demyanov, and Christie 2016; Al Rassas et al. 2020; Shao, Wu, and Li 2021). Moreover, the achievement of constructing an accurate 3D geological model is a cumbersome and challenging task (Hutahaeen, Demyanov, and Christie 2017; Zhang et al. 2016). Furthermore, the DCA approach (Zhang et al. 2016; Wachtmeister et al. 2017) can predict the hydrocarbon (H.C) production rate by assessing the long-term H.C production data. In addition, the DCA approach employed the empirical equations to match the historical production volumes with different models, including exponential, hyperbolic, and harmonic models (Tomomi 2000). The applications of artificial intelligence (AI) in the oil and gas industries have grown very dramatically (Alkinani et al. 2019; Dela Torre, Gao, and Macinnis-Ng 2021), specifically, in predicting oil production (Ahmadi and Bahadori 2015; Montgomery and O'sullivan's 2017; Liu, Liu, and Gu 2020; Song et al. 2020), predicting Petrophysical properties, such as porosity and

permeability (Erofeev et al. 2019; Ahmadi and Chen 2019), optimizing well placement and oil production (Ahmadi and Bahadori 2015; Nwachukwu et al. 2018), and predicting of Pressure-Volume-Temperature (PVT) properties (El-Sebakhy 2009).

Moreover, in the literature, many studies have been presented for predicting oil production. For example, Fan et al. (2021) presented a new model by integrating Autoregressive Integrated Moving Average (ARIMA) and Long Short-Term Memory (LSTM) to predict oil production. Alalimi et al. (2021) presented an optimized Random Vector Functional Link (RVFL) for time series forecasting for Tahe oilfield, China. Liu, Liu, and Gu (2020) and Song et al. (2020) employed LSTM-based models to predict oil production using historical production datasets. Sagheer and Kotb (2019) introduced an efficient deep learning approach called DLSTM to overcome the cumbersome of conventional forecasting tools. Zhang and Hu (2021) introduced a new forecasting model using Multivariate Time Series (MTS) and Vector Autoregressive (VAR) to predict the oil production for water flooding reservoirs. Also, in (Wang, Song, and Li 2018), the authors developed a hybrid forecasting model by employing the Nonlinear Metabolism Gray Model (NMGM) and ARIMA.

The Adaptive Neuro-Fuzzy Inference System (ANFIS) is a well-known technique that has been employed in different applications, including time-series prediction and forecasting applications, such as wind speed prediction (Liu, Tian, and Li 2015), river flow prediction (Belvederesi et al. 2020) air-overpressure prediction (Harandizadeh and Armaghani 2021) and others (Asl, Masomi, and Tajbakhsh 2020; Betiku et al. 2016; Singh et al. 2020). However, the conventional ANFIS model faces some shortcomings in its parameters configuration. The configuration process is very important and it has significant impacts on the quality of solutions as well as the training process. Thus, the applications of optimization methods can enhance the configuration process.

In this paper, we propose a modified Aquila Optimizer (AO) (Abualigah et al. 2021) using the Opposition-Based Learning (OBL), called AOOBL, to optimize ANFIS parameters and to boost its forecasting accuracy. In general, the AO algorithm has a high exploitation ability. However, its ability to explore the search space needs more improvements, so we use the OBL. The developed model, AOOBL-ANFIS, is applied to forecast oil production from different oilfields. In the developed AOOBL optimization algorithm, the OBL is employed to enhance the traditional AO algorithm's search process and avoid trapping at local optima. We used real-world oil production datasets from two different countries, China and Yemen, to evaluate the proposed AOOBL-ANFIS

model. Additionally, we applied several modified ANFIS models using well-known optimization algorithms to assess the performance of the AOOBL method.

In this study, our main contributions are:

- An efficient time-series forecasting approach, called AOOBL-ANFIS, to forecast oil production based on historical production data.
- A new variant of the AO algorithm based on the OBL technique, which is used to boost the performance of the AO algorithm.
- Enhance the performance of the traditional ANFIS model by using the developed AOOBL algorithm.
- Evaluate the developed model with real-world data collected from two well-known oilfields in China and Yemen. More so, we compare the applications of several optimization algorithms to the proposed AOOBL-ANFIS, such as the ANFIS model, Particle Swarm Optimization (PSO)-ANFIS, Genetic Algorithm (GA)-ANFIS, Sine Cosine Algorithm (SCA)-ANFIS, Slime Mold Algorithm (SMA)-ANFIS, Grey Wolf Optimizer (GWO) – ANFIS and Aquila Optimizer (AO)-ANFIS.

The rest sections of the study paper are presented as follows. A number of related works are presented in Section 2. The preliminaries of the ANFIS, AO, and OBL are given in Section 3. The description of the developed AOOBL-ANFIS model is introduced in Section 4. Section 5 presents the evaluation experiments. The conclusion is presented in Section 6.

2. Related work

2.1. Different oil production forecasting techniques

In this section, we recap a number of the recently proposed methods employed for forecasting oil production.

Singh, Seol, and Myshakin (2021) introduced a new method that could predict gas hydrate saturation (S_h) for any well by using different settings such as bulk density, porosity, compressional wave (P wave) velocity well-logs neural networks. The study results revealed that the accuracy of the developed methods in prediction S_h was 83%. Al-Shabandar et al. (2021) proposed a new forecasting model to predict oil production using a deep Gated Recurrent Unit (GRU). The employed GRU comprises several hidden layers, in which each layer has a set of nodes. The proposed model has a simple structure and can identify time series datasets with

long intervals. In (Alalimi et al. 2021), an enhanced version of the Random Vector Functional Link (RVFL) using Spherical Search Optimizer (SSO) was proposed to forecast oil production. This model was evaluated with oil production datasets collected from Tahe oilfield, China. McKenna et al. (2020) studied three different forms of uncertainty, such as facies geometry, reservoir rock heterogeneity, and permeability distribution, to determine their impact on the evaluation and prediction of reservoirs. Different techniques, including Sequential Gaussian Simulation (SGS), Kriging, and probability-field (p-field), were employed to estimate previous uncertainty levels. Liu, Liu, and Gu (2020) introduced a reliable and accurate prediction model of oil production relying on empirical mode decomposition ensemble and LSTM. In (Negash and Yaw 2020), an Artificial Neural Network (ANN) based model was employed to forecast oil production, which involves a physics-based extraction of features for fluid production prediction to enhance the prediction effect. Zanjani, Salam, and Kandara (2020) used three methods to forecast oil production, including ANN, Linear Regression (LR), and Support Vector Regression (SVR). The results revealed that all three methods achieved acceptable prediction results, where the best results were obtained by the ANN method. Abdullayeva and Imamverdiyev (2019) developed an oil forecasting model using a hybrid approach of Conventional Neural Network (CNN) and LSTM. Fan et al. (2021) developed a hybrid model using ARIMA and LSTM to forecast oil production. Moreover, different methods have been utilized for oil production forecasting, including LSTM (Liu, Liu, and Gu 2019; Sagheer and Kotb 2019), nonlinear Autoregressive Exogenous Model (NARX) (Heghedus, Shchipanov, and Rong 2019), and Higher-Order Neural Network (HONN) (NC et al. 2013).

However, the applications of traditional machine learning and advanced deep learning models require more data to train the model. Therefore, the ANFIS model performs better when the size of the data is small.

2.2 Applications of ANFIS model in time series forecasting approaches

This section summarizes some of the ANFIS applications in different time series approaches and the oil industry.

Shojaei et al. (2014) applied the ANFIS model to estimate reservoir oil bubble point pressure. They used 750 time-series data collected from different locations to evaluate two modified versions of the ANFIS. Also, they compared the ANFIS to several techniques to approve its performance. Yavari et al. (2018) applied

Hareland-Rampersad and Bourgoyne and Young models with ANFIS for drilling rate prediction. They used datasets from the South Pars gas field, Iran.

Additionally, they compared this approach to several well-known rates of penetration prediction methods. They found that ANFIS-based methods outperformed other methods. Kumar (2021) investigated Karanja oil using different conditions, namely, volume, catalyst, time, oil molar ratio, and microwave power for producing biodiesel. The ANFIS was applied to the prediction and modeling processes, which showed significant performance. In (Al-Qaness, Abd Elaziz, and Ewees 2018), the Sine Cosine Algorithm (SCA) was adopted to optimize ANFIS parameters to be applied for oil consumption forecasting. This model was applied to estimate oil consumption in two countries, the USA and Canada. In (Abd Elaziz, Ewees, and Alameer 2020), a modified ANFIS method was proposed using the genetic algorithm and salp swarm algorithm. The developed ANFIS model was applied to predict crude oil prices. In (Al-qaness et al. 2019), another developed ANFIS model was proposed to forecast oil consumption in different countries. The Multi-Verse Optimizer (MVO) was applied to enhance ANFIS forecasting capability. In (Al-qaness et al. 2021), an enhanced version of the Slime Mold Algorithm (SMA) was used to optimize ANFIS. The developed ANFIS model was applied to forecast the air quality index in Wuhan City, China.

There are also different ANFIS applications in the time series prediction field. For example, Pousinho, Mendes, and Catalão (2011) proposed a modified ANFIS model to predict wind speed. They applied the particle swarm optimization algorithm for enhancing ANFIS prediction capability. Mohammadi et al. (2015) used the ANFIS model to estimate daily global radiation.

3. Preliminaries

The backgrounds of the applied methods, ANFIS model, AO algorithm, and OBL technique are described in detail in this section, as follows.

3.1. Adaptive neuro-fuzzy inference system (ANFIS)

In 1993, Jang (1993) proposed the ANFIS model as a combination of neural networks and fuzzy systems. The fuzzy system is a well-known technique that can be utilized to map the prior knowledge into constraint sets. In general, in the ANFIS model, the "IF-THEN rules" can be used to generate a mapping for the inputs and outputs. They are identified as the "Takagi-Sugeno inference model".

Figure 1 shows the basic structure of the ANFIS model. The inputs of Layer 1 are represented by x and y . The output of the node i is represented by O_{1i} . The ANFIS model can be represented as follows:

$$O_{1i} = \mu_{A_i}(x), i = 1, 2, O_{1i} = \mu_{B_{i-2}}(y), i = 3, 4 \quad (1)$$

$$\mu(x) = e^{-\left(\frac{x-\mu_i}{\alpha_i}\right)^2} \quad (2)$$

here, μ represents the generalized Gaussian membership function, where A_i and B_i are the membership values of μ . Additionally, the premise parameter set is represented by α_i and ρ_i .

The output of the second layer can be formulated as:

$$O_{2i} = \mu_{A_i}(x) \times \mu_{B_{i-2}}(y) \quad (3)$$

The third layer output can be defined as:

$$O_{3i} = \bar{w}_i \frac{\omega_i}{\sum_{(i=1)}^2 \omega_i} \quad (4)$$

w_i is the i th output from the second layer.

Moreover, the output of the fourth layer is computed as:

$$O_{4i} = \bar{w}_i f_i = \bar{w}_i(p_i x + q_i y + r_i) \quad (5)$$

where f represents a function, which depends on the input of the network (i.e. x and y) and its parameters. r_i , q_i , and p_i are consequent parameters of the i node.

Lastly, the output of the fifth layer is generated using F and \bar{w}_i (that is defined in Equation (4)) and this is formulated in Equation (6):

$$O_{5i} = \sum_i \bar{w}_i f_i \quad (6)$$

3.2. Aquila Optimizer (AO)

The basic formulation of the Aquila Optimizer (AO) (Abualigah et al. 2021) is introduced in this section. In general, AO algorithm simulates the

social behavior of Aquila to catch its prey in nature. Similar to other Metaheuristic (MH) techniques, AO is a population-based optimization technique that started by forming the initial population X that has N agents. This process has been performed using the following equation.

$$X_{ij} = r_1 \times (UB_j - LB_j) + LB_j, i = 1, 2, \dots, N, j = 1, 2, \dots, Dim \quad (7)$$

where UB_j and LB_j are limits of the search domain. $r_1 \in [0, 1]$ is a random value and Dim is the dimension of the agent.

The next step of the AO technique is to perform either exploration and exploitation until finding the optimal solution. Followed (Abualigah et al. 2021), two strategies are used to conduct exploration and exploitation.

The first strategy is used to perform the exploration depending on using the best agent X_b and the average of agents (X_M). The mathematical formulation of this strategy is given as:

$$X_i(t+1) = X_b(t) \times \left(1 - \frac{t}{T}\right) + (X_M(t) - X_b(t) \times rand), \quad (8)$$

$$X_M(t) = \frac{1}{N} \sum_{i=1}^N X(t), \quad j = 1, 2, \dots, Dim \quad (9)$$

In Equation (8), $(1 - \frac{t}{T})$ controls the search during the exploration phase. T denotes the maximum number of iterations, and $rand$ refers to a random value between 0 and 1.

In addition, the second strategy uses the Levy flight ($Levy(D)$) distribution and X_b to update the exploration ability of the solutions, and this strategy is formulated as:

$$X_i(t+1) = X_b(t) \times Levy(D) + X_R(t) + (y - x) \times rand \quad (10)$$

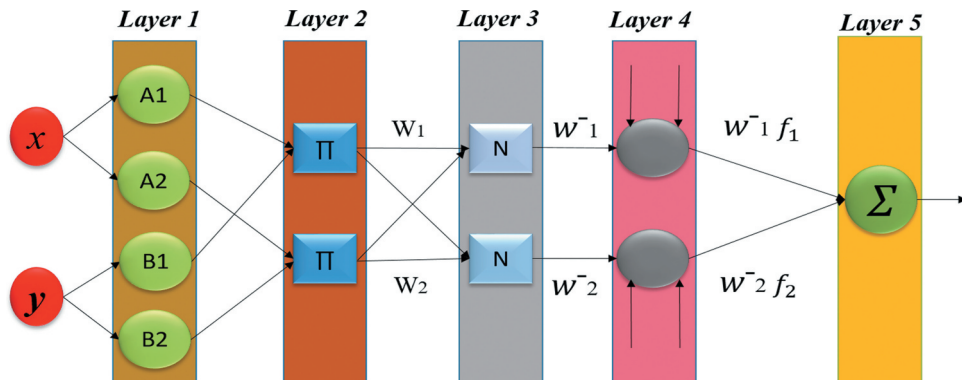


Figure 1. The basic ANFIS structure.

$$Levy(D) = s \times \frac{u \times \sigma}{|v|^{\frac{1}{\beta}}}, \sigma = \left(\frac{\Gamma(1 + \beta) \times \text{sine}\left(\frac{\pi\beta}{2}\right)}{\Gamma\left(\frac{1+\beta}{2}\right) \times \beta \times 2^{\left(\frac{\beta-1}{2}\right)}} \right) \quad (11)$$

where $s = 0.01$ and $\beta = 1.5$, while u and v are random values, and Γ is a constant value. In Equation (10), X_R is an agent randomly selected. Moreover, y and x are applied to emulate the spiral shape, and they are formulated as:

$$y = r \times \cos \theta, x = r \times \sin \theta \quad (12)$$

$$r = r_2 + U \times D_1, \theta = -\omega \times D_1 + \theta_1, \theta_1 = \frac{3 \times \pi}{2} \quad (13)$$

where $\omega = 0.005$ and $U = 0.00565$. $r_2 \in [0, 20]$ denotes a random value, and D_1 refers to integer numbers from 1 to the length of search space.

In (Abualigah et al. 2021), the first strategy is applied to update agents inside the exploitation phase depending on X_b and X_M , similar to exploration, and it is formulated as:

$$X_i(t+1) = (X_b(t) - X_M(t)) \times \alpha - rand + ((UB - LB) \times rand + LB) \times \delta \quad (14)$$

where α and δ represent the exploitation adjustment parameters. $rand \in [0, 1]$ is a random value.

In the second strategy of exploitation, the agent can be updated using X_b , $Levy$, and the quality function QF . The mathematical definition of this strategy is given as:

$$X_i(t+1) = QF \times X_b(t) - (G_1 \times X(t) \times rand) - G_2 \times Levy(D) + rand \times G_1 \quad (15)$$

$$QF(t) = t^{\frac{2 \times rand() - 1}{(1-T)^2}} \quad (16)$$

In which $rand()$ refers to a function that generates random values. Additionally, G_1 indicates different motions that are employed for tracking the best individual solution, as in the following equation:

$$G_1 = 2 \times rand() - 1, \quad (17)$$

$rand$ indicates a random value. More so, G_2 indicates decreasing values from 2 to 0, and it is computed as:

$$G_2 = 2 \times \left(1 - \frac{t}{T}\right) \quad (18)$$

Algorithm 1 shows the fundamental steps of the AO algorithm.

Algorithm 1. Aquila Optimizer (AO);

```

1: Input: Determine the number of solutions  $N$ , total
   number of iterations  $T$ , and dimension of each
   solution Dim.
2: Set the initial value for the parameters of the AO.
3: Generate initial population  $X$ .
4: while (The end condition is not met) do
5:   Compute the fitness values for each  $X_i$ .
6:   Find the best individual  $X_b(t)$ 
7:   for ( $i = 1, 2 \dots, N$ ) do
8:     if  $t \leq \left(\frac{2}{3}\right) * T$ 
9:       Update the  $X_i$  using Equation (8).
10:      if the Fitness function  $(Fit)(X_1(t+1)) <$ 
          $Fit(X(t))$  then
11:         $X(t) = (X_1(t+1))$ 
12:        if  $Fit(X_1(t+1)) < Fit(X_b(t))$  then
13:           $X_b(t) = X_1(t+1)$ 
14:        end if
15:      end if
16:      Update the  $X_i$  using Equation (10).
17:      if  $Fit(X_2(t+1)) < Fit(X(t))$  then
18:         $X(t) = (X_2(t+1))$ 
19:        if  $Fit(X_2(t+1)) < Fit(X_b(t))$  then
20:           $X_b(t) = X_2(t+1)$ 
21:        end if
22:      end if
23:    else
24:      Update the  $X_i$  using Equation (14).
25:      if  $Fit(X_3(t+1)) < Fit(X(t))$  then
26:         $X(t) = (X_3(t+1))$ 
27:        if  $Fit(X_3(t+1)) < Fit(X_b(t))$  then
28:           $X_b(t) = X_3(t+1)$ 
29:        end if
30:      end if
31:      Update  $X_i$  using Equation (15).
32:      if  $Fit(X_4(t+1)) < Fit(X(t))$  then
33:         $X(t) = (X_4(t+1))$ 
34:        if  $Fit(X_4(t+1)) < Fit(X_b(t))$  then
35:           $X_b(t) = X_4(t+1)$ 
36:        end if
37:      end if
38:    end if
39:  end for
40: end while
41: Output return ( $X_b$ ).

```

3.3. Opposition-based learning (OBL)

Tizhoosh (2005) proposed the OBL as a machine intelligence technique. OBL received wide attention, and it has been adopted in various applications as a search mechanism to boost the performance of

different optimization algorithms (Ewees, Abd Elaziz, and Houssein 2018). It creates new opposition solutions based on current solutions to improve the search process.

To formulate the OBL, suppose X^O is an opposite value for the real value. Then, $X \in [LB, UB]$ is computed as:

$$X^O = UB + LB - X \quad (19)$$

The opposite value: the $X = (X_1, X_2, \dots, X_n)$ is a value in the search space, X_1, X_2, \dots, X_D and $X_j \in [UB_j, LB_j], j \in 1, 2, \dots, D$. This can be employed as in Equation (20):

$$X_j^O = UB_j + LB_j - X_j, \text{ where } j = 1 \dots D. \quad (20)$$

Moreover, in the optimization process, X^O and X solutions are evaluated using the fitness functions. Thereafter, the best solution is reserved, and the other one is ignored.

4. Proposed AOOBL-ANFIS model

Within this section, the developed AOOBL-ANFIS model used to predict oil production is introduced. The parameters of ANFIS are updated using the modified AOOBL algorithm that enhances the performance of the traditional AO technique.

The first step is to divide the time-series data of oil production into two sets, namely training and testing tests. The training set contains 70% of all data samples, and the testing set has 30% of the total samples. More so, the number of clusters can be defined by the Fuzzy C-Mean (FCM) to build the ANFIS.

Then, a set of solutions X is generated and using each of them to constrict the ANFIS network. Then applying the training set to the ANFIS based on X_i and compute the predicted output (P) of the training with evaluating it using the following equation:

$$MSE = \frac{1}{N_a} \sum_{i=1}^{N_s} (T_i - P_i)^2 \quad (21)$$

In Equation (21), P is the predicted output, T is the real data, N_a the total number of training samples, and N_s refers to the sample length.

Third, the developed AOOBL is employed to update the current population X by using the operators of the AO algorithm and the OBL operators in Equation (19). The OBL technique is only applied in the exploration phase due to its computational cost. After that, the terminal condition is checked; updating steps will be repeated if the condition is not satisfied. Otherwise, the best configuration X_b will be returned. Finally, the testing set is applied to the best

configuration X_b by determining the weights between Layers 4 and 5. In addition to assess the model quality for oil production time-series data. The steps of the developed AOOBL-ANFIS are presented in Figure 2.

5. Experimental evaluation

5.1. Study areas

5.1.1. Sunah oilfield, Yemen

Masila oilfield is situated in the Hadramout region, in the south part of Yemen, and is considered the most productive onshore oilfield (Lashin, Marta, and Khamis 2016). Block-14 is located in the Masila oilfield with a total area of 1250 km². Block-14 consists of several oilfields, including Tawila, Sunah, N- Sunah, Camaal, N-Camaal, etc. Sunah oilfield is located in the Northeast corner of Masila oilfield. Sunah oilfield is the second-largest oilfield in Block-14, and it is subdivided into three reservoirs, namely S1, S2, and S3. Moreover, S1 is a sandstone reservoir, and it consists of three main reservoir units, namely S1A, S1B, and S1C; however, S1A is the target area of this study (Hakimi et al. 2017; Al-Areeq and Maky 2015).

5.1.2. Block 9, Tahe Oilfield, China

The location of Block-9, Tahe oilfields is situated in Tahe oilfield, Luntai region, Xinjiang province, China. It was explored in the 1990s by China National Petroleum Corporation (CNPC) with a total proven reserve of 600 × 106 tones. Taha oilfield is divided into several, including block-9. Block-9 is placed at east longitude as 84°13'9"-84°18'52" degree, and north latitude as 41°15'56"~41°16'4, nearly 60 km southwest of Luntai region of Xinjiang, China (Wu et al. 2018).

5.2. Performance metrics

Four evaluation metrics are employed in this study as shown in Table 1, namely, Mean Absolute Error (MAE), Root Mean Square Error (RMSE), Standard deviation (Std), and Coefficient of Determination R^2 . Where \bar{Y} is the mean of Y , also Y and P_y are output and its predicted value.

5.3. Results

5.3.1. Masila oilfields, Yemen

First, we evaluate the proposed AOOBL-ANFIS using the production datasets of Masila oilfields, Yemen. More so, we considered several models to be

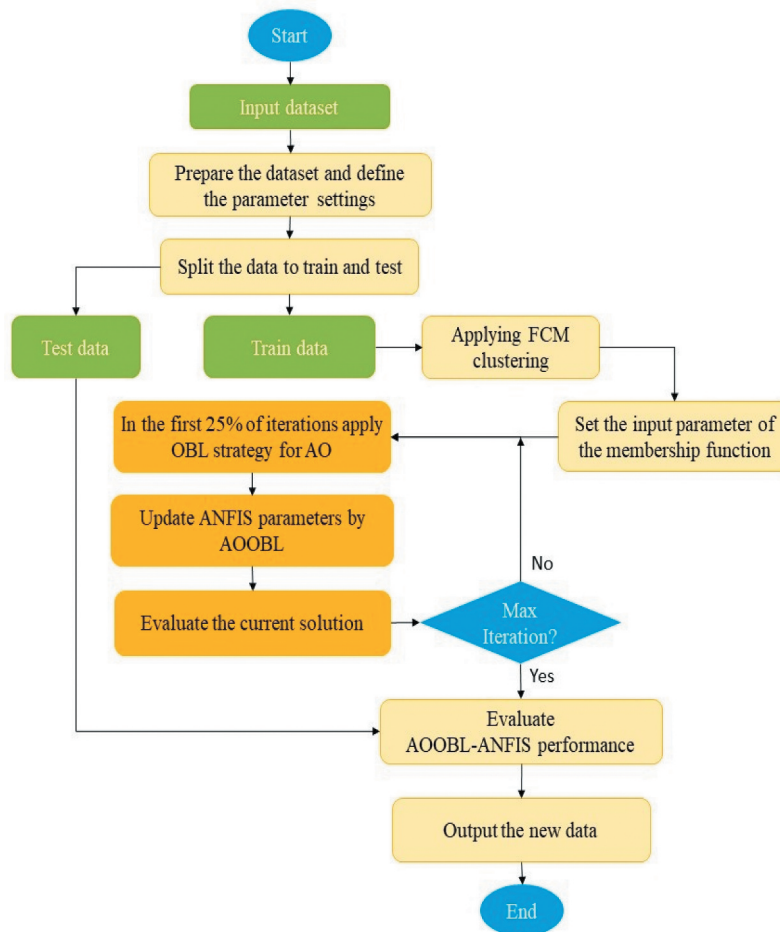


Figure 2. Workflow of the developed AOOBL-ANFIS.

Table 1. Evaluation metrics.

Performance metric	Definition
MAE	$MAE = \frac{1}{N_s} \sum_{i=1}^{N_s} Py_i - Y_i $
RMSE	$RMSE = \sqrt{\frac{1}{N_s} \sum_{i=1}^{N_s} (Py_i - y_i)^2}$
R^2	$R^2 = 1 - \frac{\sum_{i=1}^n (Y_i - Py_i)^2}{\sum_{i=1}^n (Y_i - \bar{Y})^2}$
Standard deviation (Std)	$Std = \sqrt{\frac{1}{N} \sum_{k=1}^N (Y_k - \bar{Y})^2}$

compared the proposed AOOBL-ANFIS, including the conventional ANFIS, in addition to several modified ANFIS models using well-known optimization algorithms, such as the traditional AO algorithm, Particle Swarm Optimization algorithm (PSO), sine

cosine algorithm (SCA), genetic algorithm (GA), gray wolf optimization algorithm (GWO), and slime mold algorithm (SMA).

Table 2 records the results of all models in terms of RMSE, MAE, Std, R^2 , and the computation time. We can see that the AOOBL-ANFIS achieved the best RMSE value, followed by AO-ANFIS, GA-ANFIS, PSO-ANFIS, SMA-ANFIS, GWO-ANFIS, SCA-ANFIS, and the conventional ANFIS model, respectively. The AOOBL-ANFIS also got the best MAE value, where AO-ANFIS obtained the second rank. Other models came in the following order, GA-ANFIS, PSO-ANFIS, SMA-ANFIS, GWO-ANFIS, SCA-ANFIS, and conventional ANFIS model. More so, the AOOBL-ANFIS achieved the best R^2 value of 0.957, and three models obtained the second rank, AO-ANFIS, GA-ANFIS, and PSO-ANFIS. The SMA-ANFIS obtained the fourth rank, followed by GWO-ANFIS, SCA-ANFIS, and the conventional ANFIS model. Also, the AOOBL came in the first rank in terms of Std, followed by AO-ANFIS, GA-ANFIS, PSO-ANFIS, the conventional ANFIS model, GWO-ANFIS, SMA-ANFIS, and SCA-ANFIS. Furthermore, the AOOBL-ANFIS outperformed other models in terms of computation time.

Table 2. Results of Sunah oilfields. (Bold indicates the best results).

	RMSE	MAE	R^2	Std	Optimization time
ANFIS	286.157	200.912	0.896	21.024	-
AOOBL	131.360	76.502	0.957	1.714	31.017
AO	132.666	77.447	0.956	2.859	69.428
SMA	144.034	82.938	0.951	40.913	75.629
GA	133.055	78.287	0.956	3.464	101.814
PSO	133.280	78.405	0.956	3.998	88.428
GWO	149.961	87.405	0.949	32.602	131.020
SCA	210.291	119.967	0.930	140.354	116.825

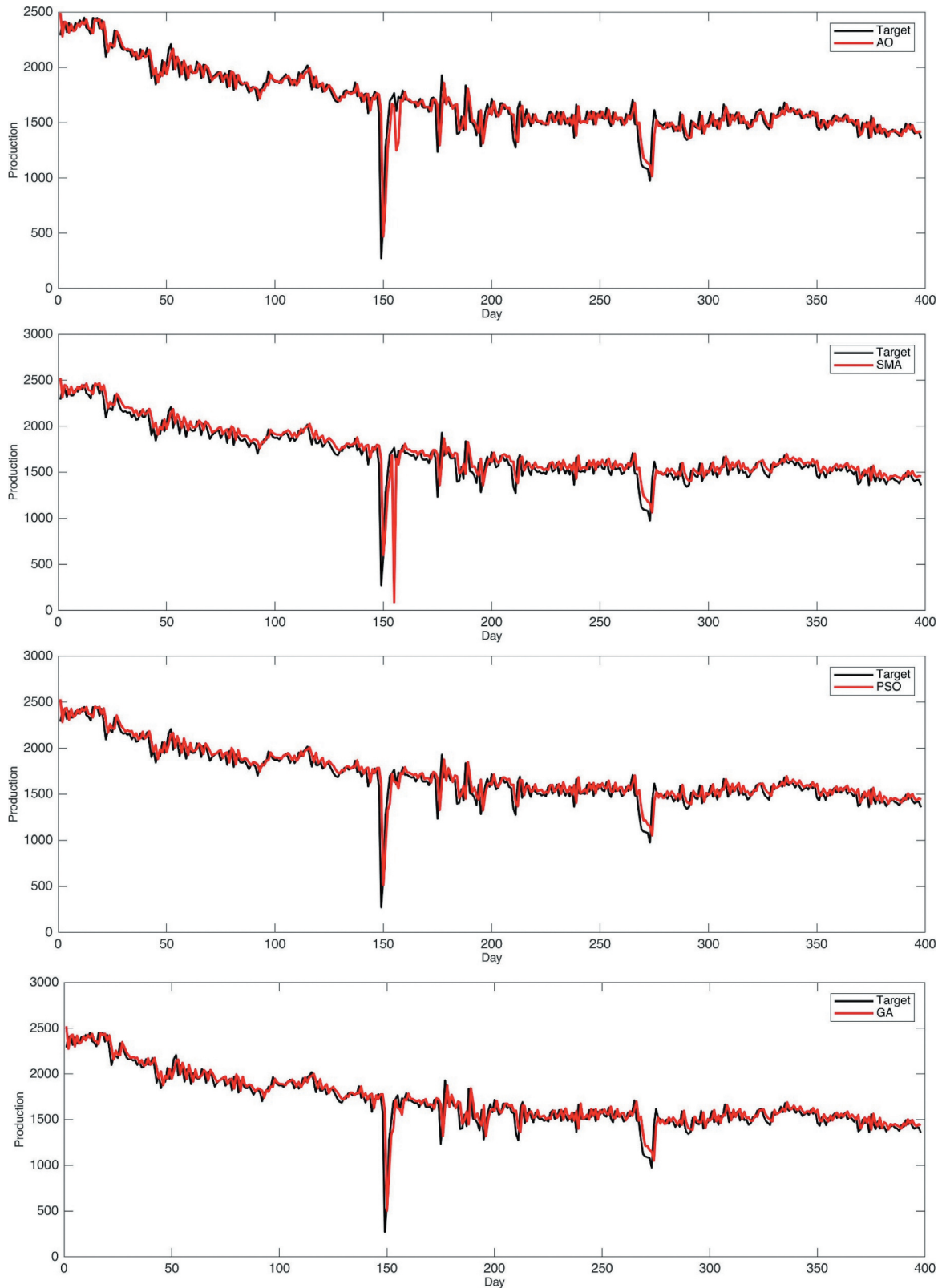


Figure 3. Prediction results of Sunah oilfields datasets.

Furthermore, Figure 3 shows the results of oil production prediction of the AOOBL-ANFIS against other compared models. It is clear that AOOBL-ANFIS is better than other models with the nearest values to the original data.

5.3.2. Results of Tahe oilfield

In this section, we evaluate the AOOBL-ANFIS using oil production data for 10 wells in Tahe oilfield, China. Table 3 tabulated the results of all compared models in terms of RMSE. The proposed

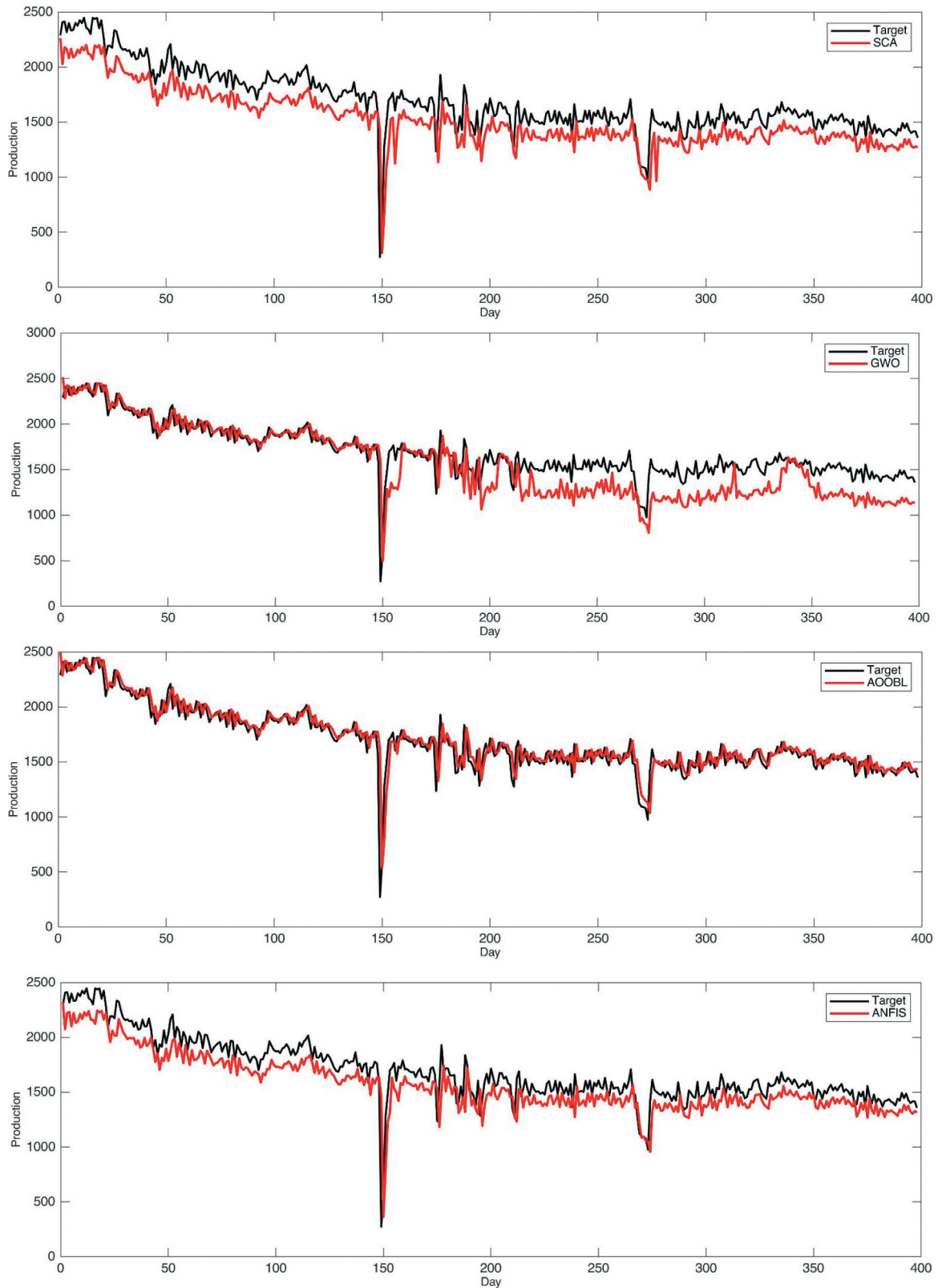


Figure 3. Continued.

AOOBL-ANFIS outperformed other compared models in terms of RMSE values in nine wells. Where in Well 10, the PSO-ANFIS obtained the first rank.

In terms of MAE value, as illustrated in Table 4, the AOOBL-ANFIS also obtained the best (smallest) MAE values in nine out of ten oil wells data. The PSO-ANFIS obtained the best MAE value in one out of

Table 3. The results of 10 oil wells, Tahe oilfield, China, in terms of RMSE. (Bold indicates the best results).

Station	ANFIS	AOOBL	AO	SMA	PSO	GA	SCA	GWO
Well 1	0.821	0.644	0.646	0.778	0.653	0.671	1.866	0.844
Well 2	0.915	0.833	0.847	0.889	0.853	0.848	1.412	0.875
Well 3	0.199	0.176	0.178	0.192	0.233	0.211	0.334	0.209
Well 4	0.926	0.831	0.832	0.872	0.832	0.834	1.106	0.847
Well 5	1.317	1.274	1.275	1.274	1.285	1.286	1.306	1.318
Well 6	0.369	0.274	0.279	0.304	0.336	0.341	0.315	0.291
Well 7	0.811	0.583	0.589	0.599	0.591	0.591	0.630	0.593
Well 8	0.235	0.115	0.118	0.141	0.134	0.140	0.233	0.137
Well 9	0.378	0.315	0.323	0.330	0.329	0.340	0.546	0.327
Well 10	1.233	1.133	1.135	1.142	1.132	1.135	1.283	1.146

ten. The AO-ANFIS came in the second rank in the average MAE values for all wells. Additionally, Table 5 shows the R^2 values of all compared models in all 10 wells. As shown from this table, AOOBL-ANFIS obtained the best R^2 in nine out of ten wells data, where the PSO-ANFIS obtained the best R^2 value for one well (Well 10).

Additionally, Figure 4 shows the prediction results of the AOOBL-ANFIS against the compared model. As noticed from this figure, the proposed AOOBL-ANFIS achieved the nearest values to the target data.

5.4. Statistical tests

For further assessments for the proposed AOOBL-ANFIS, we performed the Friedman test to highlight the differences between the proposed model and other compared models. The Friedman test is a type of non-parametric test. It is widely applied

Table 4. The results of 10 oil wells, Tahe oilfield, China, in terms of MAE. (Bold indicates the best results).

Station	ANFIS	AOOBL	AO	SMA	PSO	GA	SCA	GWO
Well 1	0.527	0.328	0.341	0.464	0.362	0.389	1.571	0.542
Well 2	0.568	0.488	0.522	0.537	0.530	0.522	0.992	0.523
Well 3	0.148	0.119	0.129	0.145	0.207	0.173	0.255	0.149
Well 4	0.599	0.393	0.395	0.406	0.399	0.401	0.644	0.407
Well 5	0.687	0.597	0.636	0.641	0.640	0.650	0.657	0.638
Well 6	0.247	0.148	0.156	0.181	0.263	0.267	0.158	0.169
Well 7	0.423	0.292	0.296	0.301	0.320	0.329	0.305	0.302
Well 8	0.207	0.080	0.085	0.110	0.108	0.114	0.193	0.106
Well 9	0.253	0.211	0.212	0.235	0.231	0.247	0.401	0.221
Well 10	0.726	0.634	0.632	0.633	0.629	0.655	0.769	0.632

Table 5. The results of 10 oil wells, Tahe oilfield, China, in terms of R^2 . (Bold indicates the best results).

Station	ANFIS	AOOBL	AO	SMA	PSO	GA	SCA	GWO
Well 1	0.8691	0.8949	0.8948	0.8817	0.8938	0.8937	0.7582	0.8699
Well 2	0.9107	0.9248	0.9226	0.9173	0.9198	0.9226	0.8445	0.9166
Well 3	0.8872	0.9116	0.9114	0.9055	0.9116	0.9115	0.8367	0.8784
Well 4	0.9203	0.9301	0.9298	0.9232	0.9292	0.9291	0.8990	0.927
Well 5	0.9721	0.9742	0.9741	0.9739	0.9735	0.9734	0.9733	0.9722
Well 6	0.6983	0.7782	0.7780	0.7290	0.7758	0.7753	0.6782	0.7370
Well 7	0.9244	0.9633	0.9632	0.9620	0.9630	0.9632	0.9563	0.9611
Well 8	0.6012	0.7445	0.7431	0.7220	0.7402	0.7401	0.6426	0.7148
Well 9	0.9549	0.9665	0.9672	0.9666	0.9672	0.9668	0.9387	0.9647
Well 10	0.9306	0.9418	0.9411	0.9398	0.9418	0.9413	0.9335	0.9397

to detect differences between methods over multiple test runs. It ranks the methods and provides rank values for them, which can help determine the proposed method's effectiveness.

Table 6 lists the Friedman test for Sunah oilfields data. As shown from the table, the AOOBL obtained the best results. Additionally, Table 7 lists the results of the Friedman test for Tahe oilfield data. Also, the AOOBL-ANFIS recorded the best results in nine wells, where the PSO-ANFIS obtained the best results in Well 10.

6. Discussion

In this section, we also present further discussions to elaborate the performance of the developed AOOBL-ANFIS. For example, Figures 5 and 6 shows the spot plot of all compared methods for Sunah oilfields, Yemen and Well 1 of Tahe oilfield, China, respectively. It is clear that the AOOBL has significant performance compared to other optimizers.

Moreover, we compare the developed AOOBL-ANFIS to several well-known methods used for time series forecasting in literature, namely, ARIMA, LSTM, Seasonal Autoregressive Integrated Moving Average (SARIMA), and Neural Network (NN).

Table 8 shows the comparison results for all compared models for Sunah oilfield datasets. It is clear that the proposed AOOBL-ANFIS model obtained the best results in terms of RMSE, MAE, and R^2 . The ARIMA model came in the second rank, followed by SARIMA, LSTM, and NN, respectively.

Table 9 displays the results of the compared time series methods for Well 1 in Tahe oilfields datasets. Also, the results in the table indicate that the developed AOOBL-ANFIS obtained the best performance in all measures, RMSE, MAE, and R^2 . The NN came in the second rank, followed by SARIMA, LSTM, and ARIMA, respectively.

In summary, according to the evaluation experiments, we conclude that the application of the AOOBL has a significant impact on the performance of the conventional ANFIS model. Moreover, the OBL also enhanced the performance of the

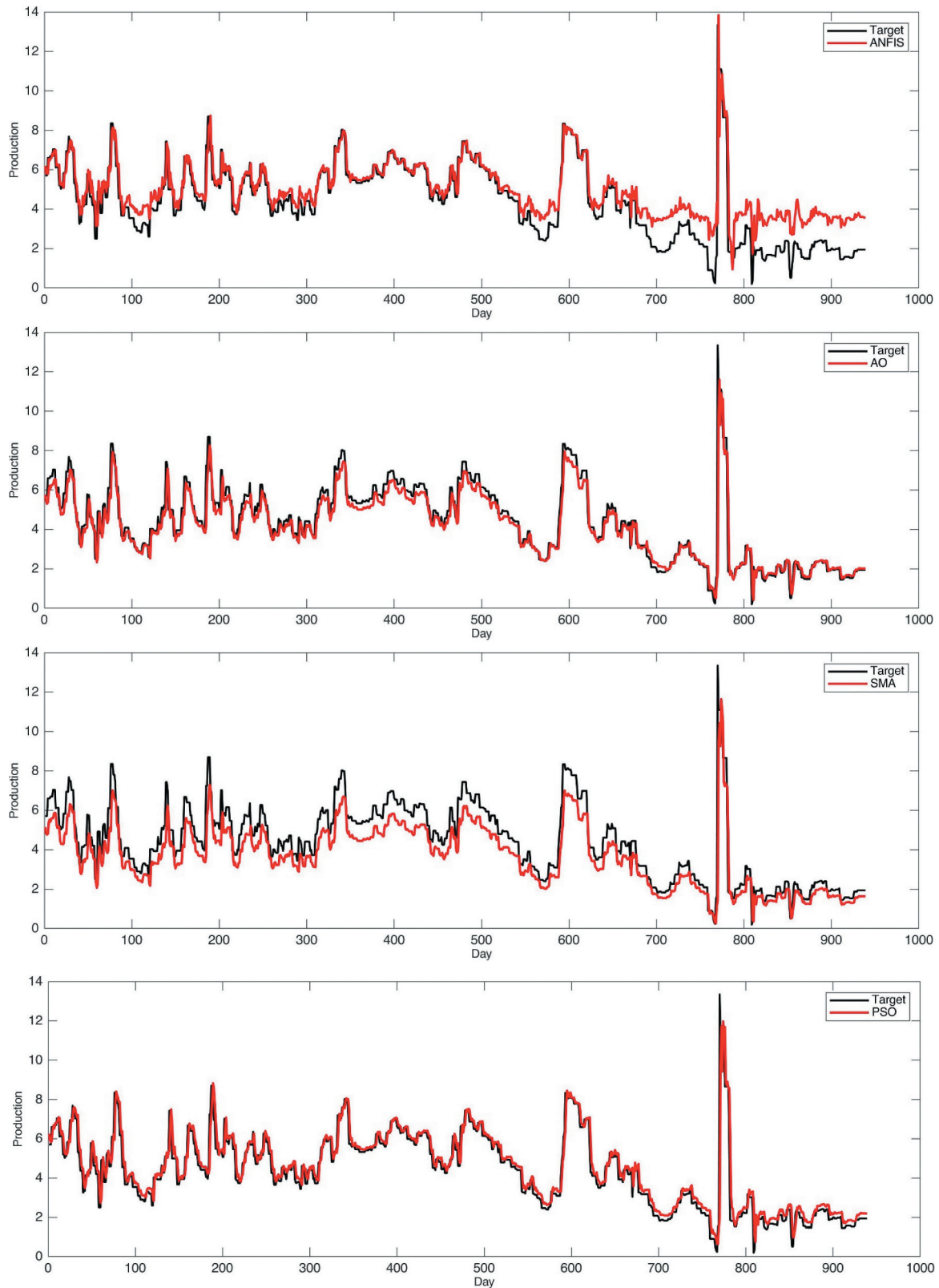


Figure 4. Prediction results of Well 1, Tahe oilfields.

traditional AO algorithm since the AOOBL-ANFIS outperformed the AOOBL-ANFIS model. However, the developed AOOBL-ANFIS has some limitations that influence its performance. For example,

determining the ratio of solutions that will be updated using the OBL is a critical parameter that causes an increase in the time complexity of the developed method.



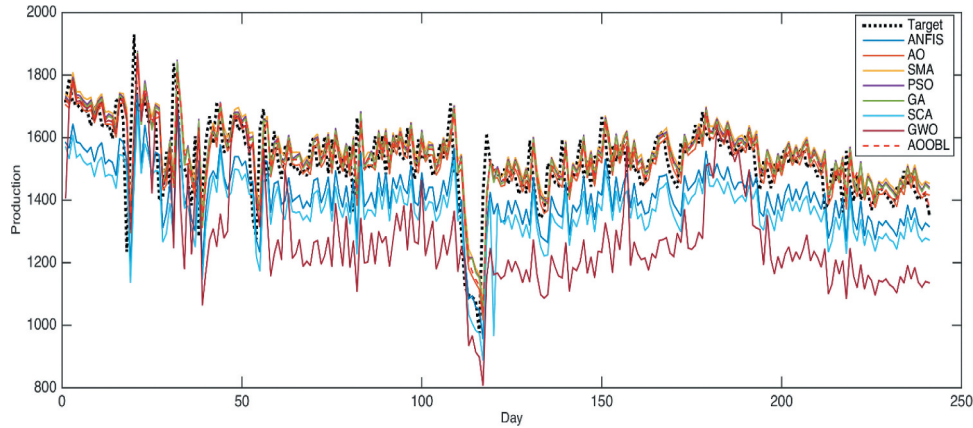
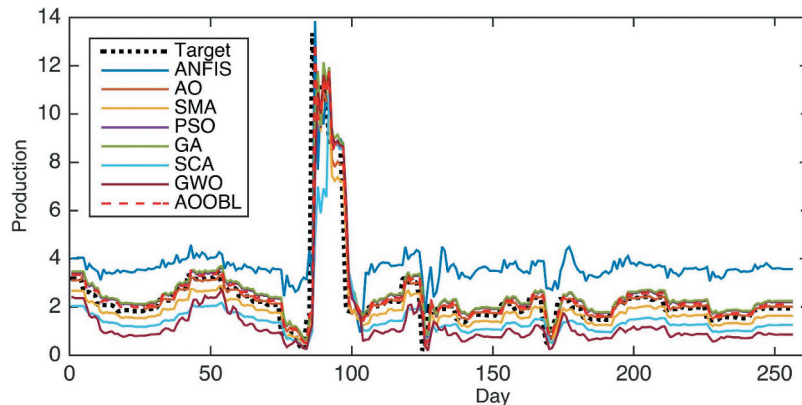
Figure 4. Continued.

Table 6. The results of the Friedman test for the Sunah oilfield dataset. (Bold indicates the best results).

	AOOBL	AO	ANFIS	SMA	PSO	GA	SCA	GWO
Sunah oilfield	2.300	5.000	6.867	4.267	3.667	3.700	4.667	5.533

Table 7. The results of the Friedman test for Tahe oilfields dataset using RMSE measure. (Bold indicates the best results).

Station	AOOBL	AO	ANFIS	SMA	PSO	GA	SCA	GWO
Well 1	1.643	2.786	6.000	4.643	4.143	3.500	7.643	5.643
Well 2	2.214	3.143	7.071	4.786	4.429	3.214	5.929	5.214
Well 3	2.429	3.500	4.857	4.214	6.286	4.214	5.643	4.857
Well 4	2.071	3.214	7.429	3.500	3.786	4.571	6.643	4.786
Well 5	2.643	3.071	7.643	3.071	5.286	5.429	5.786	3.071
Well 6	1.857	1.929	7.000	4.286	6.071	5.929	5.000	3.929
Well 7	1.929	3.143	8.000	5.000	3.786	4.643	5.500	4.000
Well 8	1.929	2.071	7.571	4.000	4.286	4.857	6.429	4.857
Well 9	1.643	2.429	7.214	4.857	4.500	5.500	5.857	4.000
Well 10	2.286	4.214	7.643	5.929	2.357	2.143	6.214	5.214

**Figure 5.** Spot plot of all methods for Sunah oilfields datasets.**Figure 6.** Spot plot of all methods for Well 1, Tahe oilfields datasets.**Table 8.** Comparison to state-of-art methods results for Yemen oilfields. (Bold indicates the best results).

Model	RMSE	MAE	R^2
LSTM	161.26	109.58	0.9512
ARIMA	139.25	82.25	0.9541
AOOBL	131.36	76.50	0.9570
SARIMA	148.68	86.05	0.9430
NN	184.23	113.84	0.9523

Table 9. Comparison to state-of-art methods results for Well 1, Tahe oilfields. (Bold indicates the best results).

Model	RMSE	MAE	R^2
LSTM	0.7101	0.4071	0.8830
ARIMA	0.7551	0.3914	0.8701
AOOBL	0.6443	0.3284	0.8950
SARIMA	0.6987	0.3387	0.8718
NN	0.6536	0.3327	0.8942

7. Conclusions

This study proposed a modified ANFIS model as a time-series forecasting approach for oil production. The traditional ANFIS was developed using an enhanced version of the Aquila Optimizer (AO) based on OBL technique. The developed model, AOOBL-ANFIS, was evaluated with different real-world oil production datasets collected from Masilah oilfield (Yemen) and Tahe oilfields (China). Also, it was compared to the conventional ANFIS model, and a modified ANFIS model using the conventional AO algorithm (AO-ANFIS), in addition to several modified ANFIS, namely, PSO-ANFIS, SMA-ANFIS, GA-ANFIS, SCA-ANFIS, and GWO-ANFIS. More so, it was compared to other well-known models, such as

ARIMA, SARIMA, LSTM, and NN. We applied several performance evaluation metrics, including RMSE, MAE, Std, and computational time to assess the performance of the AOOBL-ANFIS and the compared models. Experimental results have verified the outstanding performance of the developed AOOBL-ANFIS. We concluded that the AOOBL-ANFIS has significantly improved the conventional ANFIS performance. Additionally, we concluded that the OBL has a significant impact on the performance of the AOOBL-ANFIS compared to the conventional AO that was applied to modify the ANFIS model (AO-ANFIS) since the OBL boosted the search process of the conventional AO algorithm.

According to the significant performance of the AOOBL-ANFIS, it could be utilized in other time-series forecasting applications. Also, the AOOBL optimization method could be employed in other optimization tasks, such as image processing, cloud and fog computing, and others.

Data availability

The data that support the findings of this study are available from the corresponding author upon reasonable request.

Disclosure statement

No potential conflict of interest was reported by the author(s).

Funding

This work was supported by National Natural Science Foundation of China (Grant No. 62150410434), National Key Research and Development Program of China (Grant No. 2019YFB1405600), and by LIESMARS Special Research Funding.

Notes on contributors

Mohammed A. A. Al-qaness received the B.S., M.S., and Ph.D. degrees from the Wuhan University of Technology, in 2010, 2014, and 2017, respectively, all in information and communication engineering. He was an Assistant Professor with the School of Computer Science, Wuhan University, Wuhan, China. He is also a Postdoctoral Follower with the State Key Laboratory for Information Engineering in Surveying, Mapping, and Remote Sensing, Wuhan University. His current research interests include wireless sensing, mobile computing, data mining, machine learning, signal and image processing, and natural language processing.

Ahmed A. Ewees received the Ph.D. degree from Damietta University, Egypt, in 2012. He currently works as an Associate Professor of computer science with Damietta University. He co-supervises master's and Ph.D. students, as well as leading and supervising various graduation projects. He has many scientific research papers published in international journals and conferences. His research interests include machine

learning, artificial intelligence, text mining, natural language processing, image processing, and metaheuristic optimization techniques.

Hong Fan received the B.S. and M.S. degrees in computer science, in 1988 and 1991, respectively, and the Ph.D. degree in GIS and remote sensing from Wuhan University, China, in 2001. She is currently a Professor and the Ph.D. Supervisor with Wuhan University. She is also a Geographic Information System Expert. She has been involved in teaching and research in cartography and geographic information system for a long time. Her research interests include high-performance geographical computing, smart geographic information service, qualitative geographic information retrieval, spatial-temporal big data mining, and natural language spatial information processing.

Ayman Mutahar AlRassas received the B.S. in petroleum engineering, in 2015, from UCSI University, Malaysia. He received his master's degree in Oil and Natural Gas Engineering, from Faculty of Earth Resources, China University of Geosciences (Wuhan), China. Currently, he is doing his Ph.D. in Oil-Gas field development engineering at China University of Petroleum (East China), and his current research is about Enhanced Oil Recovery (CO₂-EOR), Carbon capture and storage (CCS), and unconventional resources.


Mohamed Abd Elaziz received the B.S. and M.S. degrees in computer science and the Ph.D. degree in mathematics and computer science from Zagazig University, Egypt, in 2008, 2011, and 2014, respectively. From 2008 to 2011, he was an Assistant Lecturer with the Department of Computer Science. He is currently an Associate Professor with Zagazig University. He has authored or coauthored more than 100 articles. His research interests include metaheuristic technique, cloud computing machine learning, signal processing, image processing, and evolutionary algorithms.

ORCID

Mohammed A. A. Al-qaness  <http://orcid.org/0000-0002-6956-7641>

Ahmed A. Ewees  <http://orcid.org/0000-0002-0666-7055>

Hong Fan  <http://orcid.org/0000-0003-4518-8775>

Ayman Mutahar AlRassas  <http://orcid.org/0000-0002-7539-1865>

Mohamed Abd Elaziz  <http://orcid.org/0000-0002-7682-6269>

References

- Abd Elaziz, M., A.A. Ewees, and Z. Alameer. 2020. "Improving Adaptive Neuro-fuzzy Inference System Based on a Modified Salp Swarm Algorithm Using Genetic Algorithm to Forecast Crude Oil Price." *Natural Resources Research* 29 (4): 2671–2686. doi:10.1007/s11053-019-09587-1.
- Abdullayeva, F., and Y. Imamverdiyev. 2019. "Development of Oil Production Forecasting Method Based on Deep Learning." *Statistics, Optimization & Information Computing* 7 (4): 826–839. doi:10.19139/soic-2310-5070-651.

- Abualigah, L., D. Yousri, M. Abd Elaziz, A.A. Ewees, M. A. Al-qaness, and A.H. Gandomi. 2021. "Aquila Optimizer: A Novel Meta-heuristic Optimization Algorithm." *Computers & Industrial Engineering* 157: 107250. doi:10.1016/j.cie.2021.107250.
- Ahmadi, M.A., and A. Bahadori. 2015. "A LSSVM Approach for Determining Well Placement and Conning Phenomena in Horizontal Wells." *Fuel* 153: 276–283. doi:10.1016/j.fuel.2015.02.094.
- Ahmadi, M.A., and Z. Chen. 2019. "Comparison of Machine Learning Methods for Estimating Permeability and Porosity of Oil Reservoirs via Petro-physical Logs." *Petroleum* 5 (3): 271–284. doi:10.1016/j.petlm.2018.06.002.
- Al Rassas, A., S. Ren, R. Sun, A. Zafar, S. Moharam, Z. Guan, A. Ahmed, et al. 2020. "Application of 3D Reservoir Geological Model on Es1 Formation, Block Nv32, Shenvsi Oilfield, China." *Open Journal of Yangtze Oil and Gas* 5 (2): 54–72. doi:10.4236/ojogas.2020.52006.
- Alalimi, A., L. Pan, M.A. Al-Qaness, A.A. Ewees, X. Wang, and M. Abd Elaziz. 2021. "Optimized Random Vector Functional Link Network to Predict Oil Production from Tahe Oil Field in China." *Oil & Gas Science and Technology-Revue d'IFP Energies Nouvelles* 76: 3. doi:10.2516/ogst/2020081.
- Al-Areeq, N.M., and A.F. Maky. 2015. "Organic Geochemical Characteristics of Crude Oils and Oil-source Rock Correlation in the Sunah Oilfield, Masila Region, Eastern Yemen." *Marine and Petroleum Geology* 63: 17–27. doi:10.1016/j.marpetgeo.2015.01.017.
- Alkinani, H.H., A.T. Al-Hameedi, S. Dunn-Norman, R. E. Flori, M.T. Alsaba, and A.S. Amer. 2019. "Applications of Artificial Neural Networks in the Petroleum Industry: A Review." Paper presented at the SPE Middle East Oil and Gas Show and Conference, Manama, Bahrain, SPE-195072-MS. doi:10.2118/195072-MS.
- Al-Qaness, M.A., M. Abd Elaziz, and A.A. Ewees. 2018. "Oil Consumption Forecasting Using Optimized Adaptive Neuro-fuzzy Inference System Based on Sine Cosine Algorithm." *IEEE Access* 6: 68394–68402. doi:10.1109/ACCESS.2018.2879965.
- Al-qaness, M.A., M. Abd Elaziz, A.A. Ewees, and X. Cui. 2019. "A Modified Adaptive Neuro-fuzzy Inference System Using Multi-verse Optimizer Algorithm for Oil Consumption Forecasting." *Electronics* 8 (10): 1071. doi:10.3390/electronics8101071.
- Al-Qaness, M.A., H. Fan, A.A. Ewees, D. Yousri, and M. Abd Elaziz. 2021. "Improved ANFIS Model for Forecasting Wuhan City Air Quality and Analysis COVID-19 Lockdown Impacts on Air Quality." *Environmental Research* 194: 110607. doi:10.1016/j.envres.2020.110607.
- Al-Shabandar, R., A. Jaddoa, P. Liatsis, and A.J. Hussain. 2021. "A Deep Gated Recurrent Neural Network for Petroleum Production Forecasting." *Machine Learning with Applications* 3: 100013. doi:10.1016/j.mlwa.2020.100013.
- Asl, S.M.H., M. Masomi, and M. Tajbakhsh. 2020. "Hybrid Adaptive Neuro-fuzzy Inference Systems for Forecasting Benzene, Toluene & M-xylene Removal from Aqueous Solutions by HZSM-5 Nano-zeolite Synthesized from Coal Fly Ash." *Journal of Cleaner Production* 258: 120688. doi:10.1016/j.jclepro.2020.120688.
- Belvederesi, C., J.A. Dominic, Q.K. Hassan, A. Gupta, and G. Achari. 2020. "Predicting River Flow Using an AI-based Sequential Adaptive Neuro-fuzzy Inference System." *Water* 12 (6): 1622. doi:10.3390/w12061622.
- Betiku, E., V.O. Odude, N.B. Ishola, A. Bamimore, A. S. Osunleke, and A.A. Okeleye. 2016. "Predictive Capability Evaluation of RSM, ANFIS and ANN: A Case of Reduction of High Free Fatty Acid of Palm Kernel Oil via Esterification Process." *Energy Conversion and Management* 124: 219–230. doi:10.1016/j.enconman.2016.07.030.
- Cancelliere, M., F. Verga, and D. Viberti. 2011. "Benefits and Limitations of Assisted History Matching." Paper presented at the SPE Offshore Europe Oil and Gas Conference and Exhibition, Aberdeen, UK, SPE-146278-MS. doi:10.2118/146278-MS.
- Chong, K.L., K.D. Kanniah, C. Pohl, and K.P. Tan. 2017. "A Review of Remote Sensing Applications for Oil Palm Studies." *Geo-spatial Information Science* 20: 184–200. doi:10.1080/10095020.2017.1337317.
- Cumming, G. 2013. "Understanding the New Statistics: Effect Sizes, Confidence Intervals, and Meta-analysis." *Routledge*. doi:10.4324/9780203807002.
- Dela Torre, D.M.G., J. Gao, and C. Macinnis-Ng. 2021. "Remote Sensing-based Estimation of Rice Yields Using Various Models: A Critical Review." *Geo-spatial Information Science* 1–24. doi:10.1080/10095020.2021.1936656.
- El-Sebakhy, E.A. 2009. "Forecasting PVT Properties of Crude Oil Systems Based on Support Vector Machines Modeling Scheme." *Journal of Petroleum Science and Engineering* 64 (1–4): 25–34. doi:10.1016/j.petrol.2008.12.006.
- Erofeev, A., D. Orlov, A. Ryzhov, and D. Koroteev. 2019. "Prediction of Porosity and Permeability Alteration Based on Machine Learning Algorithms." *Transport in Porous Media* 128 (2): 677–700. doi:10.1007/s11242-019-01265-3.
- Ewees, A.A., M. Abd Elaziz, and E.H. Houssein. 2018. "Improved Grasshopper Optimization Algorithm Using Opposition-based Learning." *Expert Systems with Applications* 112: 156–172. doi:10.1016/j.eswa.2018.06.023.
- Fan, D., H. Sun, J. Yao, K. Zhang, X. Yan, and Z. Sun. 2021. "Well Production Forecasting Based on ARIMA-LSTM Model considering Manual Operations." *Energy* 220: 119708. doi:10.1016/j.energy.2020.119708.
- Haider, W.H. 2020. "Estimates of Total Oil & Gas Reserves in the World, Future of Oil and Gas Companies and Smart Investments by E & P Companies in Renewable Energy Sources for Future Energy Needs." Paper presented at the International Petroleum Technology Conference, Dhahran, Kingdom of Saudi Arabia, IPTC-19729-MS. doi:10.2523/IPTC-19729-MS.
- Hakimi, M.H., B.A. Al Qadasi, Y. Al Sharrabi, O.T. Al Sorore, and N.G. Al Samet. 2017. "Petrophysical Properties of Cretaceous Clastic Rocks (Qishn Formation) in the Sharyoof Oilfield, Onshore Masila Basin, Yemen." *Egyptian Journal of Petroleum* 26 (2): 439–455. doi:10.1016/j.ejpe.2016.06.004.
- Harandizadeh, H., and D.J. Armaghani. 2021. "Prediction of Air-overpressure Induced by Blasting Using an ANFIS-PNN Model Optimized by GA." *Applied Soft Computing* 99: 106904. doi:10.1016/j.asoc.2020.106904.
- Heghedus, C., A. Shchipanov, and C. Rong. 2019. "Advancing Deep Learning to Improve Upstream Petroleum Monitoring." *IEEE Access* 7: 106248–106259. doi:10.1109/ACCESS.2019.2931990.
- Hutahaean, J., V. Demyanov, and M. Christie. 2016. "Many-objective Optimization Algorithm Applied to History Matching." Paper presented at 2016 IEEE Symposium Series on Computational Intelligence (SSCI), 1–8. Athens, Greece. doi:10.1109/SSCI.2016.7850215.

- Hutahaean, J., V. Demyanov, and M.A. Christie. 2017. "On Optimal Selection of Objective Grouping for Multiobjective History Matching." *SPE Journal* 22 (4): 1296–1312. doi:10.2118/185957-PA.
- Jang, J.S. 1993. "ANFIS: Adaptive-network-based Fuzzy Inference System." *IEEE Transactions on Systems, Man, and Cybernetics* 23 (3): 665–685. doi:10.1109/21.256541.
- Kumar, S. 2021. "Production and Optimization from Karanja Oil by Adaptive Neuro-fuzzy Inference System and Response Surface Methodology with Modified Domestic Microwave." *Fuel* 296: 120684. doi:10.1016/j.fuel.2021.120684.
- Lashin, A., E.B. Marta, and M. Khamis. 2016. "Characterization of the Qishn Sandstone Reservoir, Masila Basin–Yemen, Using an Integrated Petrophysical and Seismic Structural Approach." *Journal of African Earth Sciences* 115: 121–142. doi:10.1016/j.jafrearsci.2015.11.026.
- Liu, H., H.Q. Tian, and Y.F. Li. 2015. "Comparison of New Hybrid FEEMD-MLP, FEEMD-ANFIS, Wavelet Packet-MLP and Wavelet Packet-ANFIS for Wind Speed Predictions." *Energy Conversion and Management* 89: 1–11. doi:10.1016/j.enconman.2014.09.060.
- Liu, W., W.D. Liu, and J. Gu. 2019. "Petroleum Production Forecasting Based on Machine Learning." Paper Presented at the 2019 3rd International Conference on Advances in Image Processing, 124–128. Chengdu China. doi:10.1145/3373419.3373421.
- Liu, W., W.D. Liu, and J. Gu. 2020. "Forecasting Oil Production Using Ensemble Empirical Model Decomposition Based Long Short-Term Memory Neural Network." *Journal of Petroleum Science and Engineering* 189: 107013. doi:10.1016/j.petrol.2020.107013.
- McKenna, S.A., A. Akhriev, D.E. Ciaurri, and S. Zhuk. 2020. "Efficient Uncertainty Quantification of Reservoir Properties for Parameter Estimation and Production Forecasting." *Mathematical Geosciences* 52 (2): 233–251. doi:10.1007/s11004-019-09810-y.
- Mohammadi, K., S. Shamshirband, C.W. Tong, K. A. Alam, and D. Petković. 2015. "Potential of Adaptive Neuro-fuzzy System for Prediction of Daily Global Solar Radiation by Day of the Year." *Energy Conversion and Management* 93: 406–413. doi:10.1016/j.enconman.2015.01.021.
- Montgomery, J.B., and F.M. O'sullivan. 2017. "Spatial Variability of Tight Oil Well Productivity and the Impact of Technology." *Applied Energy* 195: 344–355. doi:10.1016/j.apenergy.2017.03.038.
- NC, C.C., K.Y. Song, D.N. Saraf, and M.M. Gupta. 2013. "Production Forecasting of Petroleum Reservoir Applying Higher-order Neural Networks (HONN) with Limited Reservoir Data." *International Journal of Computer Applications* 975: 8887. doi:10.5120/12466-8834.
- Negash, B.M., and A.D. Yaw. 2020. "Artificial Neural Network Based Production Forecasting for a Hydrocarbon Reservoir under Water Injection." *Petroleum Exploration and Development* 47 (2): 383–392. doi:10.1016/S1876-3804(20)60055-6.
- Nwachukwu, A., H. Jeong, M. Pyrcz, and L.W. Lake. 2018. "Fast Evaluation of Well Placements in Heterogeneous Reservoir Models Using Machine Learning." *Journal of Petroleum Science and Engineering* 163: 463–475. doi:10.1016/j.petrol.2018.01.019.
- Nwaobi, U., and G. Anandarajah. 2018. "Parameter Determination for a Numerical Approach to Undeveloped Shale Gas Production Estimation: The UK Bowland Shale Region Application." *Journal of Natural Gas Science and Engineering* 58: 80–91. doi:10.1016/j.jngse.2018.07.024.
- Pousinho, H.M.I., V.M.F. Mendes, and J.P.D.S. Catalão. 2011. "A Hybrid PSO–ANFIS Approach for Short-term Wind Power Prediction in Portugal." *Energy Conversion and Management* 52 (1): 397–402. doi:10.1016/j.enconman.2010.07.015.
- Sagheer, A., and M. Kotb. 2019. "Time Series Forecasting of Petroleum Production Using Deep LSTM Recurrent Networks." *Neurocomputing* 323: 203–213. doi:10.1016/j.neucom.2018.09.082.
- Shao, Z., W. Wu, and D. Li. 2021. "Spatio-temporal-spectral Observation Model for Urban Remote Sensing." *Geospatial Information Science* 24 (3): 372–386. doi:10.1080/10095020.2020.1864232.
- Shojaei, M.J., E. Bahrami, P. Barati, and S. Riahi. 2014. "Adaptive Neuro-fuzzy Approach for Reservoir Oil Bubble Point Pressure Estimation." *Journal of Natural Gas Science and Engineering* 20: 214–220. doi:10.1016/j.jngse.2014.06.012.
- Singh, H., Y. Seol, and E.M. Myshakin. 2021. "Prediction of Gas Hydrate Saturation Using Machine Learning and Optimal Set of Well-logs." *Computational Geosciences* 25 (1): 267–283. doi:10.1007/s10596-020-10004-3.
- Singh, N.K., Y. Singh, A. Sharma, and E. Abd Rahim. 2020. "Prediction of Performance and Emission Parameters of Kusum Biodiesel Based Diesel Engine Using Neuro-fuzzy Techniques Combined with Genetic Algorithm." *Fuel* 280: 118629. doi:10.1016/j.fuel.2020.118629.
- Song, X., Y. Liu, L. Xue, J. Wang, J. Zhang, J. Wang, L. Jiang, and Z. Cheng. 2020. "Time-series Well Performance Prediction Based on Long Short-Term Memory (LSTM) Neural Network Model." *Journal of Petroleum Science and Engineering* 186: 106682. doi:10.1016/j.petrol.2019.106682.
- Tizhoosh, H.R. 2005. "Opposition-based Learning: A New Scheme for Machine Intelligence." Paper presented at International conference on computational intelligence for modelling, control and automation and international conference on intelligent agents, web technologies and internet commerce (CIMCA-IAWTIC'06), Vol. 1, 695–701. Vienna, Austria. doi:10.1109/CIMCA.2005.1631345.
- Tomomi, Y. 2000. "Non-uniqueness of History Matching." Paper presented at the SPE Asia Pacific Conference on Integrated Modelling for Asset Management, Yokohama, Japan. SPE-59434-MS. doi:10.2118/59434-MS.
- Wachtmeister, H., L. Lund, K. Aleklett, and M. Höök. 2017. "Production Decline Curves of Tight Oil Wells in Eagle Ford Shale." *Natural Resources Research* 26 (3): 365–377. doi:10.1007/s11053-016-9323-2.
- Wang, Q., X. Song, and R. Li. 2018. "A Novel Hybridization of Nonlinear Grey Model and Linear ARIMA Residual Correction for Forecasting US Shale Oil Production." *Energy* 165: 1320–1331. doi:10.1016/j.energy.2018.10.032.
- Wu, J., T. Fan, Z. Gao, Y. Gu, J. Wang, Y. Du, C. Li, et al. 2018. "Identification and Characteristic Analysis of Carbonate Cap Rock: A Case Study from the

- Lower-Middle Ordovician Yingshan Formation in Tahe Oilfield, Tarim Basin, China.” *Journal of Petroleum Science and Engineering* 164: 362–381. doi:[10.1016/j.petrol.2017.12.070](https://doi.org/10.1016/j.petrol.2017.12.070).
- Yavari, H., M. Sabah, R. Khosravanian, and D. Wood. 2018. “Application of an Adaptive Neuro-fuzzy Inference System and Mathematical Rate of Penetration Models to Predicting Drilling Rate.” *Iranian Journal of Oil and Gas Science and Technology* 7 (3): 73–100. doi:[10.22050/ijogst.2018.83374.1391](https://doi.org/10.22050/ijogst.2018.83374.1391).
- Zanjani, M.S., M.A. Salam, and O. Kandara. 2020. “Data-Driven Hydrocarbon Production Forecasting Using Machine Learning Techniques.” *International Journal of Computer Science and Information Security (IJCSIS)* 18 (6): 65–72.
- Zhang, H., D. Rietz, A. Cagle, M. Cocco, and J. Lee. 2016. “Extended Exponential Decline Curve Analysis.” *Journal of Natural Gas Science and Engineering* 36: 402–413. doi:[10.1016/j.jngse.2016.10.010](https://doi.org/10.1016/j.jngse.2016.10.010).
- Zhang, R., and J.I.A. Hu. 2021. “Production Performance Forecasting Method Based on Multivariate Time Series and Vector Autoregressive Machine Learning Model for Waterflooding Reservoirs.” *Petroleum Exploration and Development* 48 (1): 201–211. doi:[10.1016/S1876-3804\(21\)60016-2](https://doi.org/10.1016/S1876-3804(21)60016-2).